

# Local magnetization fluctuations in superconducting glasses resolved by Hall sensors

J. Lefebvre,<sup>1</sup> M. Hilke,<sup>1</sup> Z. Altounian,<sup>1</sup> K. W. West,<sup>2</sup> and L. N. Pfeiffer<sup>2</sup>

<sup>1</sup>*Department of Physics, McGill University, Montréal, Canada H3A 2T8.*

<sup>2</sup>*Bell Laboratories, Alcatel-Lucent, Murray Hill, New Jersey 07974-0636, USA*

We report on magnetization measurements performed on a series of  $\text{Fe}_x\text{Ni}_{1-x}\text{Zr}_2$  superconducting metallic glasses with  $0 \leq x \leq 0.5$  using the Hall effect of a nearby 2-dimensional electron gas (2DEG) in a GaAs/ $\text{Al}_{0.33}\text{Ga}_{0.67}\text{As}$  heterostructure as a local probe. The great sensitivity of the Hall effect of the 2DEG in such heterostructure is exploited to determine the magnetization of the superconductor due to the Meissner effect and flux trapping. The data is used to determine the lower critical field  $B_{c1}$  of the superconductors as a function of temperature. Surprisingly large fluctuations in the magnetization are also observed and attributed to the presence of large flux clusters in the superconductor.

Various techniques can be used to obtain information about the local magnetic profile in type II superconductors. Some, like muon spin rotation<sup>1,2</sup>, neutron scattering<sup>3,4</sup> or scanning tunneling microscopy<sup>5,6,7</sup>, can provide information about the ordering of vortices in the superconductor without directly probing the magnetic field. Others have either sufficient spatial resolution or sensitivity to resolve single flux quanta by directly probing the magnetic field of the vortices. These include for instance, Lorentz microscopy, magnetic force microscopy, Bitter decoration, scanning SQUID (superconducting quantum interference device) microscopy, and scanning Hall probes. Of these, scanning Hall probes offer the best balance between good sensitivity and high spatial resolution<sup>8</sup>. Since the beginning of the 1990s, the Hall resistance of the two-dimensional electron gas (2DEG) that forms at the interface between GaAs and AlGaAs in GaAs/AlGaAs heterostructures has been used to probe magnetic flux in superconductors<sup>9,10,11,12</sup>. With a sensitivity of about  $3 \times 10^{-8} \text{ T Hz}^{-1/2}$  and submicron spatial resolution<sup>8</sup>, these can be used to image the local flux profile in superconductors at low vortex density. In the past, Hall probe arrays have been successfully used to image vortices and vortex bundles in high  $T_c$  superconductors<sup>11</sup>. They were also applied to the study of local magnetic profiles<sup>13</sup> and their temporal evolution in such superconductors<sup>14,15,16</sup>. In these types of experiments, the influence of the inhomogeneous flux profile of the superconductor on the Hall effect of the nearby 2DEG can only be detected if the 2DEG-superconductor separation is very small; this maximal separation is usually approximated as the distance between vortices, and thus decreases with increasing magnetic field<sup>17</sup>. Such requirements can be quite stringent, especially in superconductors having large vortices (large penetration depth  $\lambda$ ) resulting in a magnetic profile inhomogeneity that is rapidly lost upon increase of the external magnetic field.

In this article, we show that using a 2DEG Hall probe with an active area of  $100 \times 50 \text{ } \mu\text{m}^2$  and at a distance from the superconductor's surface between 1 and 10 microns, we were able to determine the presence of large vortex clusters in some of our superconductors. A sketch of the geometry proposed for this experiment can be vi-

sualized in the upper inset of Fig. 1. In an externally applied magnetic field, screening currents are induced in the superconductor due to the Meissner effect. These currents produce the self-field of the superconductor (its magnetization) which fully (or partially) shield the interior of the superconductor from the external field. As a result, the magnetic field threading the nearby 2DEG is composed of the applied field, plus the magnetization of the superconductor. Since the vortices in these metallic glasses are quite large<sup>18,19</sup> (close to  $1 \text{ } \mu\text{m}$ ), no magnetic field inhomogeneity due to these is expected to survive at the 2DEG located over  $1 \text{ } \mu\text{m}$  away. In this case, the Hall resistance of the 2DEG reflects the average magnetic field crossing the active area of the 2DEG defined by the Hall junction; the portion of this magnetic field due to the superconductor is attributable to the Meissner effect and gives the local magnetization of the superconductor.

Performing magnetization measurements using this technique, we could determine the temperature dependence of the lower critical field  $B_{c1}$  of the superconductors. In addition, large fluctuations in the local magnetization in some of the superconductors were observed, and found to correlate with the Fe content in the superconductors. We believe that the fluctuations are caused by vortex bundles. A mechanism is proposed to account for the formation of the vortex clusters.

In detail, we use a GaAs/ $\text{Al}_{0.33}\text{Ga}_{0.67}\text{As}$  heterostructure with a 2DEG sitting 200 nm below the surface with electron density  $n_e = 1.55 \times 10^{11} \text{ cm}^{-2}$  and low-temperature mobility  $\mu = 2.86 \times 10^6 \text{ cm}^2\text{V}^{-1}\text{s}^{-1}$  to measure the low-field magnetization of a series of metallic glasses  $\text{Fe}_x\text{Ni}_{1-x}\text{Zr}_2$  with  $0 \leq x \leq 0.5$ . This yields a magnetic field sensitivity of about  $4 \text{ } \Omega/\text{mT}$ , independent of size of the Hall probe. On the contrary, the spatial resolution of the Hall probe directly depends on the active area of the 2DEG probe. Therefore, in order to define the active area, a Hall bar pattern, as shown in the lower inset of Fig. 1, was scratched on the surface of the heterostructure. The scratching is performed by a diamond tip attached to a fixed arm; the stage on which the GaAs/AlGaAs sample sits is moved horizontally and vertically by two motors as controlled by a Labview program which produces the desired Hall bar pattern. This allows

for quick and efficient patterning of 2DEG structures. Indium contacts are deposited in the contact pads of the Hall bar which is then heated to 400 °C in a sealed quartz tube under vacuum and let to diffuse for 25 minutes in order to contact the 2DEG below the surface. The superconductor is then placed over the active area confined by the scratched pattern in the GaAs/AlGaAs and held with vacuum grease. We find this technique very convenient because it allows for easy removal and exchange of the superconductor without changing degradation of the 2DEG. Also, as it cools, vacuum grease hardens and contracts and holds the superconductor well in place. The resulting distance between the 2DEG and superconductor can be estimated from the capacitance between them; doing this, we obtain this distance to be from 1 to 10  $\mu\text{m}$ , depending on the sample.

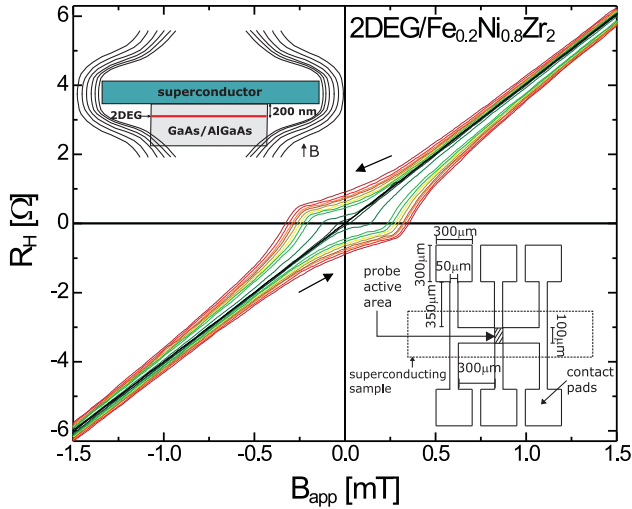


FIG. 1: Hall resistance  $R_H$  of the 2DEG with a sample of superconducting  $\text{Fe}_{0.2}\text{Ni}_{0.8}\text{Zr}_2$  nearby. From larger to smaller hysteresis loop :  $T=0.35, 0.53, 0.72, 0.88, 1.11, 1.26, 1.42, 1.57, 1.79, 2.01, 2.31$  K. Insets: (upper) Sketch of experimental geometry showing the bending of magnetic field lines due to the Meissner effect of the superconductor. (lower) Schematic representation of the Hall bar patterned on the GaAs/AlGaAs.

The  $\text{Fe}_x\text{Ni}_{1-x}\text{Zr}_2$  alloys are prepared by arc-melting appropriate concentrations of the starting elements Fe (99.9%), Ni (99.999%) and Zr (99.95%) in Ti-gettered atmosphere. Amorphous ribbons, about 20  $\mu\text{m}$  thick, are then obtained from melt-spinning in 40 kPa helium onto a copper wheel spinning at 50 m/s; the absence of crystallinity was confirmed by the absence of Bragg peaks in Cu  $K_\alpha$  x-ray diffraction patterns.

A set of 2DEG Hall resistance  $R_H$  curves acquired as a function of applied magnetic field  $B_{\text{app}}$  on a 2DEG/ $\text{Fe}_{0.2}\text{Ni}_{0.8}\text{Zr}_2$  superconductor composite sample is shown in Fig. 1. The different colored curves correspond to different temperatures as described in the caption.

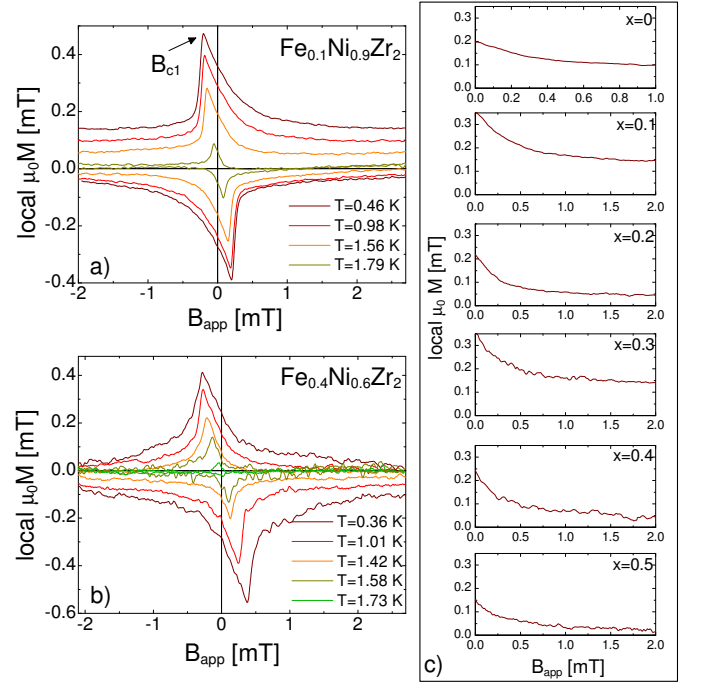


FIG. 2: Local magnetization as a function of applied magnetic field for a)  $\text{Fe}_{0.1}\text{Ni}_{0.9}\text{Zr}_2$  and b)  $\text{Fe}_{0.4}\text{Ni}_{0.6}\text{Zr}_2$  for different temperatures and c) only for  $T \approx 0.35$  K for each  $x$ .

Above the critical temperature of the superconductor  $T_c$ , the Hall resistance recovers a linear relationship to  $B_{\text{app}}$ , as it should in the absence of the superconductor. Below  $T_c$ , the total magnetic field  $B_{\text{tot}}$  threading the 2DEG is composed of  $B_{\text{app}}$ , plus the demagnetizing field of the superconductor  $\mu_0 M$ , i.e.  $\mu_0 M = B_{\text{tot}} - B_{\text{app}}$ .  $B_{\text{tot}}$  is obtained from the measured Hall resistance in the presence of the superconductor and the conversion from  $R_H$  to  $B$  field is obtained from the Hall constant measured above  $T_c$

$$B_{\text{tot}} = \frac{R_H}{dR_H/dB|_{T>T_c}}. \quad (1)$$

The Hall constant is independent of temperature, any dependence of the Hall resistance on temperature is then attributable to the contacts or to a longitudinal contribution. In our case, this longitudinal contribution due to a slight contact misalignment was found to be very small, less than 0.2  $\Omega$  at  $B=0$  and  $T=0.33$  K, and was thus neglected. The low-field local magnetization loops thus obtained are computed using the linear fit of  $R_H$  vs  $B_{\text{app}}$  for  $T > T_c$  to determine  $B_{\text{app}}$ ; results for  $\text{Fe}_x\text{Ni}_{1-x}\text{Zr}_2$  with  $x=0.1$  and  $x=0.4$  are shown in Fig. 2 a) and b).

We define the location of  $B_{c1}$  at the position of the peak in the local magnetization profile, as shown in Fig. 1a).  $B_{c1}$  values are obtained for the different superconductors  $\text{Fe}_x\text{Ni}_{1-x}\text{Zr}_2$  with  $0 \leq x \leq 0.5$  as a function of temperature, Fig. 3. Flux pinning and hysteresis, as well as surface barrier effects often render the observation of  $B_{c1}$

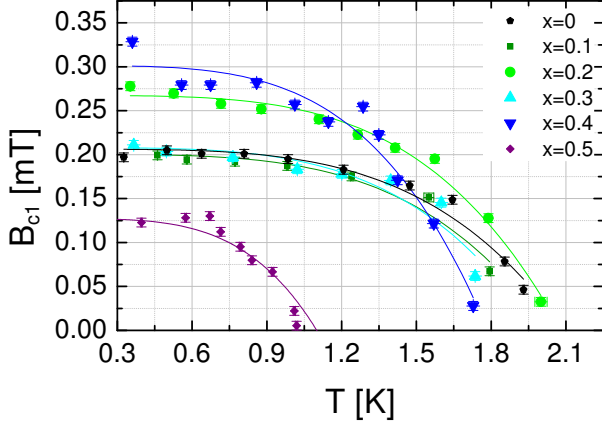


FIG. 3: Lower critical field  $B_{c1}$  as a function of temperature for different metallic glasses  $\text{Fe}_x\text{Ni}_{1-x}\text{Zr}_2$ . The lines are fits to  $B_{c1} = B_{c1}(0)(1 - (T/T_c)^4)$  based on a two-fluid model of superconductivity<sup>20</sup>.

difficult, although the weak-pinning properties of these metallic glasses and the local nature of our magnetization measurements make it possible here. Indeed, in strongly-pinned superconductors, the magnetization peak at  $B_{c1}$  is often broad and shallow<sup>21</sup>; this can be contrasted to the very sharp peak observed here. The local nature of our magnetization measurement is also responsible for this, since averaging is thus only performed over a small portion of the superconductor located in the middle of the superconductor. As a consequence of this, no demagnetizing factor needs to be taken into account for the scaling of the applied magnetic field.

A peculiarity of the magnetization data shown here is the conspicuous increase in fluctuations in the magnetization signal with increasing Fe content in the superconductors. This gradual increase in fluctuations was obtained for superconductors with Fe content  $x$  from 0 (smallest fluctuations) to  $x=0.5$  (largest fluctuations). See Fig. 2c) for a portion of the magnetization curve at  $T \simeq 0.35$  K for each superconductor measured to see this evolution. We quantify these fluctuations in magnetization by computing the relative size of fluctuations  $\frac{M - \langle M \rangle}{\langle M \rangle}$  as a function of Fe content (Fig. 4).  $\langle M \rangle$  is obtained from fitting a 4<sup>th</sup> order polynomial to the magnetization signal as necessary to determine the mean of a non-constant signal. This is computed over the four sections of the magnetization curve corresponding to both polarities of the applied field and both sweep directions; the values shown in Fig. 4 are the mean of these four evaluations for the lowest temperature probed, and the error bars the statistical error. The size of fluctuations is observed to be pretty constant with temperature for the six samples measured (see inset of Fig. 5 for  $x=0.2$ ); no particular trend is observed in  $\Delta M = M - \langle M \rangle$  as a function of temperature.

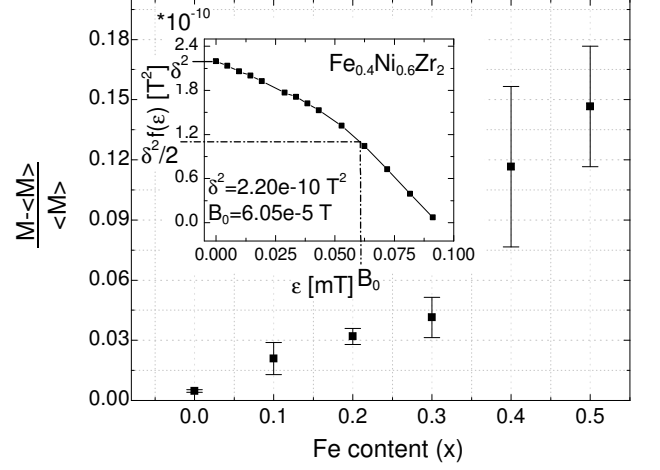


FIG. 4: a) Relative fluctuations  $\frac{M - \langle M \rangle}{\langle M \rangle}$  as a function of Fe content  $x$  in  $\text{Fe}_x\text{Ni}_{1-x}\text{Zr}_2$ . Inset: function  $f(\varepsilon)$  as described in the text as a function of magnetic field increment  $\varepsilon$ , evaluated on  $\text{Fe}_{0.4}\text{Ni}_{0.6}\text{Zr}_2$ .

Since the magnetization represents a sum over magnetic moments  $M = \sum_i^N m_i$ ,  $M$  depends on both the total number  $N = V/a^3$  of these moments, and on their magnitude  $m_i$  ( $V$  is the volume of the superconductor, and  $a^3$  is the characteristic size of grains). Accordingly, from the magnetization fluctuations, one can determine the minimum value for the size of grains and the characteristic magnetic field  $B_0$  of fluctuations. More precisely, since  $\frac{M - \langle M \rangle}{\langle M \rangle} < \frac{1}{\sqrt{N}}$ , assuming independent and maximally fluctuating grains, we obtain  $a > 13 \mu\text{m}$  for the  $x=0.5$  alloy. Furthermore, the characteristic field of fluctuations  $B_0$  can be estimated from computation of the auto-covariance function  $f(\varepsilon) = \langle M(B)M(B + \varepsilon) \rangle - \langle M(B) \rangle^2$ , where  $\varepsilon$  is a small magnetic field increment, and  $\sqrt{f(0)} = \delta = \sqrt{\langle M(B)^2 \rangle - \langle M(B) \rangle^2}$  is the usual standard deviation expression;  $B_0$  is the value of  $\varepsilon$  at which  $f(\varepsilon) = \delta^2/2$  (inset of Fig. 4). As expected,  $f(\varepsilon)$  decreases with increasing  $\varepsilon$  as correlations diminish. The characteristic magnetic flux of fluctuations can then be computed as  $\Phi = B_0 \times A$  where  $A$  is the active area of the Hall probe perpendicular to the field (Fig. 5), from which it can be deduced that the fluctuations arise due to the entry and exit of vortex bundles in and out of the area of the superconductor defined by the Hall probe. In the samples containing the largest amount of Fe, these correlated flux movements can be quite large with 70 to 80 vortices. These processes are visible because our Hall probe provides a local measurement of the magnetization and averaging of the signal is performed over only a small part of the superconductor, such effects are typically not visible in global magnetization measurements.

The occurrence of vortex movement in such large correlated bundles and its dependence on Fe content  $x$  in

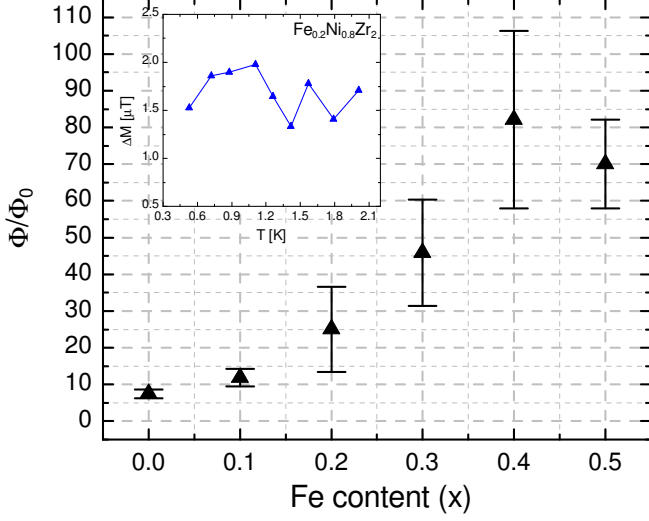


FIG. 5: Characteristic magnetic flux of fluctuations as a function of Fe content  $x$  in  $\text{Fe}_x\text{Ni}_{1-x}\text{Zr}_2$ .  $\Phi/\Phi_0$  corresponds to the number of correlated vortices entering and exiting the area of the superconductor defined by the Hall bar. As for the data of Fig. 4,  $\Phi/\Phi_0$  here is the mean of the values evaluated over the 4 sections of the magnetization curve (both field polarities and both sweep directions), and the error bars are the statistical error on the mean. Inset: Fluctuations  $\Delta M = M - \langle M \rangle$  as a function of temperature.

the superconductors can be understood as follows: The superconductor is composed of two different phases, one having weaker pinning properties than the other, such that vortex entry and exit would be privileged there. The number density and size of inhomogeneities would then increase with Fe content to yield larger fluctuations induced by larger flux bundles. Such a scenario would be consistent with the possibility that our superconducting metallic glasses are composed of Ni-rich and Fe-rich clusters having different short range order (SRO). Since Fe and Ni atoms have very similar sizes, no change in geometrical short range order (GSRO) is expected upon substitution of Ni for Fe in these alloys. This is however not necessarily true of the chemical short range order (CSRO); pertaining mainly to the atomic species of nearest-neighbors, CSRO could vary because Fe and Ni do not have the same electronic structure. This question is especially relevant in these metallic glasses because it is known that the first crystallization products of  $\text{NiZr}_2$  assume a body-centered-tetragonal (bct) structure while those of  $\text{FeZr}_2$  are face-centered-cubic (fcc), and because the atomic arrangement in the amorphous phase is assumed to be very close to that of the first crystallization products<sup>22,23</sup>, a transition in SRO with  $x$  in amorphous  $\text{Fe}_x\text{Ni}_{1-x}\text{Zr}_2$  could be expected. According to this picture, a phase having SRO resembling the fcc arrangement of  $\text{FeZr}_2$  could develop with increasing Fe content in the

alloys; most probably having different pinning properties, it could lead to vortex clustering.

Other evidences published elsewhere point to two-phase superconductivity in the alloys with large Fe content  $x=0.5$  and  $0.6$ , namely a normal-to-superconducting state transition showing a double step, and anomalous clockwise hysteresis at the  $B_{c2}$  transition<sup>18,19</sup>. If the magnetization fluctuations observed here are indeed the hallmark of a two-phase superconductor, it could lead to the interesting conclusion that a structural transition exists in these amorphous alloys, although it has not been seen before despite investigation, for instance using Mössbauer spectroscopy<sup>24</sup>. Such small differences in the atomic ordering in the amorphous state cannot be highlighted easily due to the small scale involved, but for this to take place, it means that using the small vortex core ( $\xi \simeq 7$  nm in these metallic glasses<sup>19,25</sup>) as a probe, it is possible to resolve such small changes. Considering the dramatic increase in the size of fluctuations for Fe content  $0.4 \leq x \leq 0.5$ , if a structural transition exists in these alloys, it must be located close to  $x=0.4$ , but with a gradual increase of an Fe-rich phase starting with  $x = 0.1$ .

However, it is not clear how structural inhomogeneities could lead to magnetization fluctuations as a function of magnetic field. It could be the case if the respective sizes of the Ni-rich and Fe-rich regions, or the boundary between these two phases, changed as a function of field, but this should be invariant. This picture is however consistent with the observation that  $\Delta M$  does not have a clear dependence on temperature (Fig. 5, inset), meaning that the fluctuations are issued from a phenomenon constant with respect to that variable, and not from a thermally-dependent process.

In addition, the Fe content modifies the pinning properties, which are extremely weak in these amorphous alloys. Indeed, as discussed elsewhere<sup>19,25,26</sup>, pinning in these alloys is from 10 to 1000 times weaker than in other similar superconductors<sup>27,28,29,30</sup>, with a critical current density  $J_c < 3$  A/cm<sup>2</sup> at  $B=0.15B_{c2}$ . Also, it has been shown that the pinning force decreases by almost a factor of 5 when going from the alloys with a low Fe content ( $x=0$  and  $0.1$ ) to the alloys with a high Fe content ( $x=0.5$  and  $0.6$ )<sup>19</sup>. This is partly due to the larger size of vortices ( $\lambda$  and  $\xi_{GL}$  almost double from  $x=0$  to  $x=0.6$ ) in alloys with a high Fe content<sup>18,19</sup>, which confers less efficient pinning for pinning sites of similar size. In addition, the larger size of vortices favors vortex-vortex interactions, thus enhancing collective effects, which also contributes to diminishing effective pinning. In these superconductors, it was shown that vortices arrange in the Bragg glass (BG) phase at driving forces lower than the depinning threshold and at low vortex density<sup>31</sup>, such that even at such low magnetic field ( $\lesssim 2$  mT) collective effects are significant; the existence of elastic interactions between vortices is a necessary condition for the BG phase<sup>32</sup>. Therefore, vortices will likely form correlated clusters of increasing size with Fe content, which

will induce fluctuations in the magnetization as bundles enter and exit the boundary defined by the Hall bar on the superconductor.

To summarize, we have shown that using our Hall probe, we could measure the low-field magnetization of a series of  $\text{Fe}_x\text{Ni}_{1-x}\text{Zr}_2$  metallic glass superconductors and the dependence of  $B_{c1}$  on temperature. We further observed fluctuations in the magnetization signal,

the magnitude of which increases with the Fe content in the superconductors. The origin of these fluctuations is linked to the presence of large vortex bundles in the superconductors. These fluctuations are consistent with an increasingly two-phase system (Fe-rich and Ni-rich) with different SRO and pinning properties leading to an increased effective vortex-vortex interaction which enhances collective vortex movement.

- 
- <sup>1</sup> S. L. Lee, P. Zimmermann, H. Keller, M. Warden, I. M. Savić, R. Schauwecker, D. Zech, R. Cubitt, E. M. Forgan, P. H. Kes, et al., Phys. Rev. Lett. **71**, 3862 (1993).
  - <sup>2</sup> U. Divakar, A. J. Drew, S. L. Lee, R. Gilardi, J. Mesot, F. Y. Ogrin, D. Charalambous, E. M. Forgan, G. I. Menon, N. Momono, et al., Phys. Rev. Lett. **92**, 237004 (2004).
  - <sup>3</sup> R. Cubitt, E. M. Forgan, G. Yang, S. L. Lee, D. M. Paul, H. A. Mook, M. Yethiraj, P. H. Kes, T. W. Li, A. A. Menovsky, et al., Nature **365**, 407 (1993).
  - <sup>4</sup> T. Klein, I. Joumard, S. Blanchard, J. Marcus, R. Cubitt, T. Giamarchi, and P. L. Doussal, Nature **413**, 404 (2001).
  - <sup>5</sup> I. Maggio-Aprile, C. Renner, A. Erb, E. Walker, and O. Fischer, Phys. Rev. Lett. **75**, 2754 (1995).
  - <sup>6</sup> A. M. Troyanovski, M. van Hecke, N. Saha, J. Aarts, and P. H. Kes, Phys. Rev. Lett. **89**, 147006 (2002).
  - <sup>7</sup> A. M. Troyanovski, J. Aarts, and P. H. Kes, Nature **399**, 665 (1999).
  - <sup>8</sup> S. J. Bending, Adv. Phys. **48**, 449 (1999).
  - <sup>9</sup> S. J. Bending, K. von Klitzing, and K. Ploog, Phys. Rev. B **42**, 9859 (1990).
  - <sup>10</sup> S. J. Bending, K. von Klitzing, and K. Ploog, Phys. Rev. Lett. **65**, 1060 (1990).
  - <sup>11</sup> A. Oral, S. J. Bending, and M. Henini, Applied Physics Letters **69**, 1324 (1996).
  - <sup>12</sup> S. T. Stoddart, S. J. Bending, A. K. Geim, and M. Henini, Phys. Rev. Lett. **71**, 3854 (1993).
  - <sup>13</sup> E. Zeldov, A. I. Larkin, V. B. Geshkenbein, M. Konczykowski, D. Majer, B. Khaykovich, V. M. Vinokur, and H. Shtrikman, Phys. Rev. Lett. **73**, 1428 (1994).
  - <sup>14</sup> G. Karapetrov, V. Cambel, W. K. Kwok, R. Nikolova, G. W. Crabtree, H. Zheng, and B. W. Veal, Journal of Applied Physics **86**, 6282 (1999).
  - <sup>15</sup> Y. Abulafia, A. Shaulov, Y. Wolfus, R. Prozorov, L. Burlachkov, Y. Yeshurun, D. Majer, E. Zeldov, and V. M. Vinokur, Phys. Rev. Lett. **75**, 2404 (1995).
  - <sup>16</sup> R. G. van Veen, A. H. Verbruggen, E. van der Drift, S. Radelaar, S. Anders, and H. M. Jaeger, Review of Scientific Instruments **70**, 1767 (1999).
  - <sup>17</sup> J. Rammer and A. L. Shelankov, Phys. Rev. B **36**, 3135 (1987).
  - <sup>18</sup> J. Lefebvre, Ph.D. thesis, McGill University, Montréal, Canada (2008).
  - <sup>19</sup> J. Lefebvre, M. Hilke, and Z. Altounian (2008), to be published.
  - <sup>20</sup> M. Tinkham, *Introduction to Superconductivity* (McGraw-Hill, 1996).
  - <sup>21</sup> T. H. Shen, M. Elliott, A. E. Cornish, R. H. Williams, D. Westwood, C. T. Lin, W. Y. Liang, D. A. Richie, J. E. F. Frost, and G. A. C. Jones, Superconductor Science and Technology **4**, 232 (1991).
  - <sup>22</sup> R. Wang, Nature **278**, 700 (1979).
  - <sup>23</sup> C. McKamey, D. M. Kroeger, D. S. Easton, and J. O. Scarbrough, J. Mater. Sci. **21**, 3863 (1986).
  - <sup>24</sup> M. Dikeakos, Z. Altounian, D. H. Ryan, and S. J. Kwon, J. Non-Cryst. Solids **250-252**, 637 (1999).
  - <sup>25</sup> M. Hilke, S. Reid, R. Gagnon, and Z. Altounian, Phys. Rev. Lett. **91**, 127004 (2003).
  - <sup>26</sup> J. Lefebvre, M. Hilke, R. Gagnon, and Z. Altounian, Phys. Rev. B **74**, 174509 (2006).
  - <sup>27</sup> T. G. Berlincourt, R. R. Hake, and D. H. Leslie, Phys. Rev. Lett. **6**, 671 (1961).
  - <sup>28</sup> P. H. Kes and C. C. Tsuei, Phys. Rev. B **28**, 5126 (1983).
  - <sup>29</sup> R. Wördenweber, P. H. Kes, and C. C. Tsuei, Phys. Rev. B **33**, 3172 (1986).
  - <sup>30</sup> J. M. E. Geers, C. Attanasio, M. B. S. Hesselberth, J. Aarts, and P. H. Kes, Phys. Rev. B **63**, 094511 (2001).
  - <sup>31</sup> J. Lefebvre, M. Hilke, and Z. Altounian, Phys. Rev. B **78**, 134506 (2008).
  - <sup>32</sup> T. Giamarchi and S. Bhattacharya, *Vortex phases* (2001), cond-mat/0111052v1.